JOURNAL OF MICROENCAPSULATION
2020, VOL. 37, NO. 3, 205–219
https://doi.org/10.1080/02652048.2020.1720029

Taylor & Francis
Taylor & Francis Group

ORIGINAL ARTICLE



# Microencapsulation of retinyl palmitate by melt dispersion for cosmetic application

Aditi Nandy[a], Eliza Lee[a], Abhyuday Mandal[b], Raha Saremi[a] and Suraj Sharma[a]

[a]Innovative Materials Research Group, Department of Textiles, Merchandising and Interiors, University of Georgia, Athens, GA, USA; [b]Department of Statistics, University of Georgia, Athens, GA, USA

**ABSTRACT**

Retinyl palmitate was encapsulated in wax matrix by melt dispersion for the purpose of economic and sustainable cosmeceutical formulation with minimum use of synthetic chemicals. We evaluated the effect of different process variables of microencapsulation by melt dispersion. In this study, a three level definitive screening design was applied, where the microcapsule properties were analysed through statistical analysis to understand the effect of four process variables: type of wax, theoretical loading capacity, surface concentration and stirring speed. Microparticles were characterised for size using image analysis; loading capacity and encapsulation efficiency using ultraviolet-visible spectroscopy; antioxidant activity through DPPH (2,2-diphenyl-1-picrylhydrazyl) assay. Melt dispersion method was effective to produce microcapsules with a spherical shape and mean size as small as 28 μm. The encapsulation efficiency ranged 60−80%. Theoretical loading capacity ($p$-value = 0.00232, significance level, $\alpha$ = 1%) and surfactant% ($p$ = 0.0573, $\alpha$ = 10%) were found to be the most significant factors to control the actual loading capacity and size of microcapsules.

**ARTICLE HISTORY**
Received 23 July 2019
Accepted 16 January 2020

**KEYWORDS**
Microencapsulation; melt dispersion; cosmeceuticals; cosmetic; anti-aging; retinyl palmitate; vitamin A; process variables

## Introduction

Cosmeceuticals, products that can impart beneficial results for human body signify one of the most promising sectors of the skin-care market, particularly for products that are intended to treat or inhibit the aging of the skin (Oliveira 2014). Cosmeceuticals have similar results as pharmaceutical drugs, but they are produced and marketed as cosmetics and usually sold over-the-counter. According to Zion market research (2016), the global market revenue of anti-aging products is predicted to be over USD 216 billion by 2021. Another report (360 Research Reports 2018) forecasts that the global cosmeceuticals market has been growing at a CAGR of 9.38% during the period 2018–2023 and is expected to reach to a value of USD 80.36 billion by the end of the forecast period. In this respect, vitamin A and its derivatives have great importance in the cosmeceuticals industry because they act as antioxidants as well as cell regulators, hence improve the skin texture by stimulating collagen production and reducing skin damage (Ganceviciene *et al.* 2012)

Bradley *et al.* (2015), in their review on over-the-counter anti-aging topical agents, discussed the mechanism of action of all-trans retinoic acid (t-RA) on the skin, which is shown in Figure 1(a). Extra-cellular matrix (ECM) proteins such as fibrillar collagens contribute to skin repair and regeneration (Watt and Fujiwara 2011), whereas matrix-metalloproteinase (MMP) is liable for skin degradation (Fisher *et al.* 1999). Retinoic acid prevents and treats photo-aging not only by increasing ECM deposition but also by decreasing synthesis of MMP via inhibiting the activator complex of MMP, named AP-1 (Fisher and Voorhees 1998). Thus, upon treatment with retinoids, the photoaged skin achieves a visibly improved texture and smoothness.

Retinyl palmitate (RP) ($C_{36}H_{60}O_2$), is a stable lipophilic ester of retinol and palmitic acid. Although pure retinol is more effective in anti-aging than its derivatives, it has adverse effects such as burning, redness, and peeling off the skin. On the contrary, RP has a mild and slow reaction on the skin. After being topically applied onto the skin, RP needs to be converted to retinol catalysed by enzymes within the skin, and then to active retinoic acid through oxidative processes (Boerman and Napoli 1996, Lupo 2001, Oliveira 2014). Figure 1(b) shows the schematic of this mechanism. However, there is evidence of the effectiveness

CONTACT Suraj Sharma ssharma@uga.edu Textiles, Merchandising and Interiors, University of Georgia, 352 Dawson Hall, Athens, GA 30602, USA

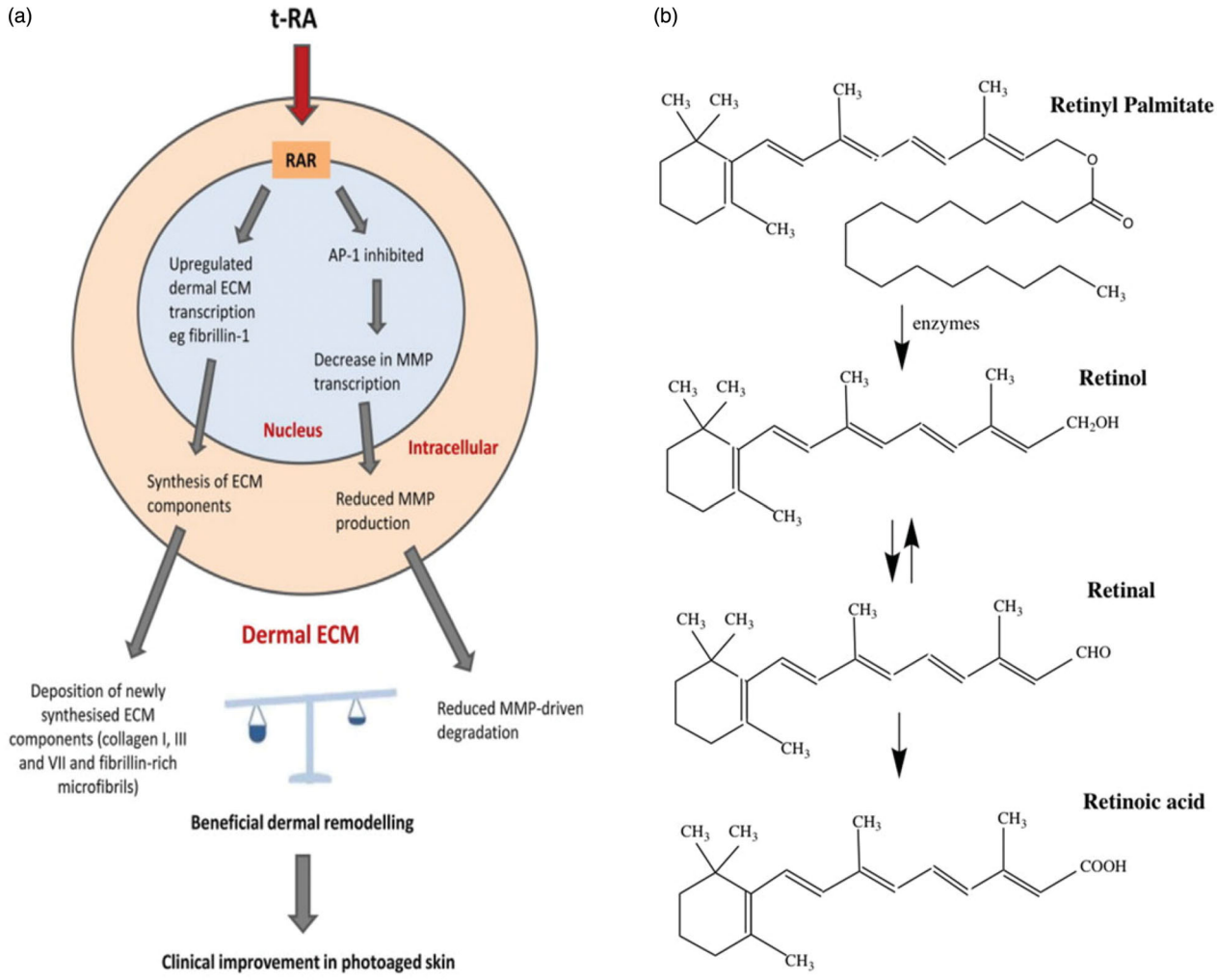


**Figure 1.** Action of retinoids on skin. (a) All-trans retinoic acid (t-RA) clinically improves the appearance of photoaged skin through increased deposition of extra-cellular matrix (ECM) through upregulating transcription as well as synthesis of ECM proteins such fibirillin-1. T-RA also contributes to the suppression of the activity of matrix metalloproteinases (MMPs) by inhibiting transcription activator complex such as AP-1, thus reduces for MMP-driven skin degradation. [permission for reusing figure obtained from Elsevier; licence number: 4596330836294]. (b) Conversion of retinyl palmitate retinoic acid is essential to be active, which is catalysed by enzymes within the skin through oxidative processes. [Adapted from: Goncalves *et al*. (2016)]

of RP as antiaging in previous studies. A study by Counts *et al*. (1988) showed that topical administration of RP in rats for 14 days resulted in an epidermal thickening with enhanced protein and collagen stimulation. In another comparison study (Duell *et al*. 1997), an increased epidermal thickness was observed in human skin as well.

From the perspective of textiles, an approximately 80% of textiles will be technical or functionalised in the next twenty years (Upadhyay *et al*. 2016). Today, cosmetic textiles, being a category of innovative textile materials, are also considered as technical textiles. A standard definition by French Textile & Apparel Industry Standardisation Office (Bureau National des Industries du Textile et de l'Habillement) states that "Cosmetic textiles are textile articles which contain a substance or preparation designed to be released over the long term onto different, superficial areas of the human body, in particular, the epidermis, and claiming one or more specific properties, such as cleansing, perfume, figure enhancement, skin protection, maintenance or anti-odor"(Saini and Manideep 2017). Cosmetotextiles are a fusion of textile substrate with cosmetic properties that can impart functionality to the skin by releasing the active ingredient. (Singh *et al*. 2011, Ömeroğullari Başyiği *et al*. 2018). Cosmetic ingredients can be from herbal, animal derivatives or synthetic and inorganic sources (Yılmaz and Öndoğan 2014).

Nowadays, many of the cosmetics, as well as personal care products, contain biologically active ingredients, which are unstable and vulnerable to environmental factors such as temperature, light, pH,

and oxygen (Casanova and Santos 2016). Microencapsulation technology increases the stability of such ingredients by providing a protective shell and releasing the core substance when triggered by different factors such as external pressure, dissolution, enzymatic degradation, abrasion, and heat (Jyothi *et al.* 2012). Microencapsulation technology encases solids, liquids, or gaseous substances in small capsules with a size range of sub-micrometer to several millimetres that can release their contents at controlled rates during application (Benita 2005, Mishra 2016). There are various microencapsulation methods; however, the selection of suitable method primarily depends on the specific application and properties of the encapsulated material. One of the widely used methods is solvent evaporation/extraction (Koo *et al.* 2008, Kim *et al.* 2010, Ito *et al.* 2013, Giri *et al.* 2013, McCall and Sirianni 2013, Barroso *et al.* 2014). In this method, the active content is dissolved, dispersed or emulsified into a polymer solution containing volatile organic solvents such as dichloromethane, chloroform or ethyl acetate, followed by their emulsification into an external aqueous or oil phase (Deshmukh *et al.* 2016, Mishra 2016). Resulting microcapsules are formed by the evaporation/extraction of the solvent. Coacervation method involves the phase separation of two immiscible liquids triggered by a change in temperature, pH, or addition of salt, resulting in one dense coacervate phase (droplets) and another dilute colloidal phase (Martins *et al.* 2009, Xiao *et al.* 2014, Salaün 2016). Ionic gelation method of microencapsulation entraps the active agent by a biopolymeric gel network such as alginate or chitosan (Yoksan et al. 2010, Jimtaisong and Saewan 2014, Mishra 2016). The spray drying method is often used to produce atomised, dry particle, where emulsion containing the ingredient and carrier is homogenised and fed into a hot spray dryer (Yin and Yates 2009, Harris *et al.* 2011). Other means of encapsulation include desolvation (Duclairoir *et al.* 2002, Banjare and Ghillare 2012), thin-film hydration (Bhalerao and Raje Harshal 2003), high-pressure homogenisation (Shigeta *et al.* 2004), coprecipitation (Yang *et al.* 2003), facile method (Irani *et al.* 2019, Irani *et al.* 2017) etc. Thus active ingredients such as essential oils, plant extracts, vitamins, and other antioxidants have been encapsulated for cosmeceutical application.

Previously vitamin A has been microencapsulated in various methods including spray drying, spray cooling, coacervation (phase separation), emulsion system, liposomes, solid lipid nanoparticles, and inclusion complexation (Goncalves *et al.* 2016). For cosmetic formulations, retinoids has been reported to be successfully encapsulated in albumin by emulsion method (Torrado *et al.* 1992), in glyceryl behenate solid lipid nanoparticles by melt solidification (Jenning *et al.* 2000), in tetraethyl orthosilicate by sol-gel encapsulation (Lee *et al.* 2001), in chitosan nanoparticles using solvent evaporation (Kim *et al.* 2006), and in maltodextrin/modified starches using spray drying method (Gangurde and Amin 2017).

Microscale particles can be multipurpose in the cosmetic formulation as well as easy to handle and incorporate into fibrous substrates. The particle size for cosmetic formulation depends on the type of application. For example, facial scrubs or exfoliators, the particles size should range from 75 to 200 μm, whereas 200−700 μm would be suitable for body scrubs (Morice 2016). On the other hand, for cosmetic textile application such as non-woven facial wipes, the capsule size should range from 1 μm to 100 μm based on the pore size of the substrate (Varona and Wright 2005).

In this study, we investigated a novel approach of melt dispersion to microencapsulate RP with a view to making the cosmetic formulation sustainable as well as cost-effective. Melt dispersion is an inexpensive and convenient method that can produce free-flowing particles with mean size range of 50–150 μm (Djordjević *et al.* 2015). This size range is suitable for cosmetic applications. Melt dispersion method has not been explored before to microencapsulate retinoids, possibly because the process involves heating and melting of encapsulation materials. However, waxes have been previously used to encapsulate bioactive compound, including heat-sensitive ones (Bodmeier *et al.* 1992). Natural waxes such as beeswax can provide anti-inflammatory, skin softening and skin healing properties, whereas carnauba wax helps provide protective skin barrier. Using natural ingredients in cosmetic formulation can provide skin benefits, without incorporating auxiliary solvents or chemicals that can have adverse side effects on sensitive skin. Other encapsulation methods such as coacervation, ionic gelation or inclusion complexation often require the use of stabilizers/crosslinking agents or expensive methods of preparation. From this perspective, in order to encapsulate active ingredient such as retinoids, melt dispersion can be an economical and eco-friendly method to impart skin- benefits of retinyl palmitate as well as natural waxes, with minimum use of synthetic chemicals.

The fundamental principle of melt dispersion method is based on the atomisation of a molten matrix

such as waxes (melting point ranging from 32 °C to 85 °C) in finely dispersed microdroplets that contain the active ingredient, followed by solidification to provide powder-like microparticles (Djordjević *et al.* 2015). In an oil-in-water emulsion system, the oil phase disperses into the continuous bulk phase to make droplets of oil surrounded by water. Surfactants reduce the interfacial tension, cage the droplets, and stabilise the droplet shape by minimising the surface area as well as surface energy (Mokhatab *et al.* 2018). As a result, spherical droplets form. A shear force such as mixing is required to break up the structure of the droplet into smaller droplets and prevent their coalescence. When the dispersion is cooled, the melted wax in the oil phase get solidified, entrapping retinyl palmitate in the matrix.

Research on microencapsulation often involves the investigation of multiple variables with a limited amount of data. Traditionally, two-level fractional factorial experiments are used for such screening designs. In this study, we used three levels to have better flexibility. More importantly, the coding of variables is used by factorial experiments, which does not make any distinction between actual levels of factors. This essentially restricts us from using actual factor levels in the analysis. Moreover, in factorial designs, some terms are often found fully confounded; and one may not be able to distinguish between the effects of certain factors and interactions. Factorial design methods require higher number of experiments to understand the main effects thoroughly. Definitive Screening design can provide estimates of main effects being unbiased by any second-order effect (Jones and Nachtsheim 2011). This design also requires a smaller number of time-consuming experiments to extract the same information as those from regular factorial or fractional factorial designs. Therefore, definitive screening designs are known to be well suited for such situations.

The overall objective of this study was to microencapsulate retinyl palmitate through melt dispersion; statistically investigate the effect of process variables such as type of wax, theoretical loading% (w/w), surfactant% (w/v) and stirring speed; and characterise the prepared microcapsules in terms of size and morphology, loading capacity, encapsulation efficiency, and antioxidant activity.

## Materials and methods

### Materials

Refined, white, beeswax pearls were purchased from Bulk Apothecary (Aurora, OH). Pure, granular paraffin wax; refined, yellow carnauba wax and retinyl palmitate (vitamin A) of 1.7 M.I.U./g. were purchased from Fisher Scientific USA (Pittsburg, PA). Tween™ 20 (Fisher BioReagents™; Pittsburg, PA), Span 85 (Sigma-Aldrich, St. Louis, MO) and Ethanol (Decon Labs, Inc., King of Prussia, PA) were used as received.

### Preparation of microcapsules

The method of preparing RP-loaded wax microcapsules by melt dispersion was developed from another study that encapsulated ethyl vanillin in carnauba wax (Milanovic *et al.* 2011). We modified the procedure based on the surfactants used, melting temperature of the materials and the levels of process variables studied. A schematic of the process of preparation is shown in Figure 2.

A vessel was filled with DI water and surfactants (a mixture of tween 20/span 85) and was heated 10 °C higher than the melting temperature of the wax. The emulsion mixture was stirred with a mechanical mixer. Simultaneously, a pre-weighed amount of wax (depending on theoretical loading% selected) was completely melted in a water bath. The melting temperature of beeswax and paraffin wax are close to 65 °C, whereas carnauba wax has a melting temperature around 86 °C. Henceforth, the heating temperature was 75 °C for beeswax and paraffin wax, while carnauba wax requires 95 °C. RP was added into the molten wax just before the mixture was poured to the vessel containing the emulsion. In this way, it was possible to ensure minimal exposure of the RP to heat. The emulsion was stirred with heat for 4 min. Then the heating was stopped, and cold DI water (at 2 °C–5 °C) was poured into the resulting dispersion in order to cool it down and to enable solidification of wax droplets. The dispersion with produced particles was cooled down spontaneously to the room temperature. Then the dispersion was vacuum filtered to collect solid wax particles and washed with ethanol and DI water to remove residual surfactants and superficial RP. Finally, the resultant particles were dried and stored in a petri dish.

Amount of wax and RP were calculated according to the theoretical loading (% w/w) and the amount of surfactant (% w/v) was calculated based on the design of the experiment. The nature of emulsion, i.e. oil in water or water in oil helps decide the selection of emulsifiers in order to attain a desired hydrophilic-lipophilic balance (HLB), a concept initially described by Griffin (1949) and later modified by Davies (1957). As Tweens (polyethoxylated sorbitan esters) are more water-soluble (HLB $>$ 10) whereas Spans (sorbitan esters) are more oil soluble (HLB $<$ 9), often a blend of both are used.

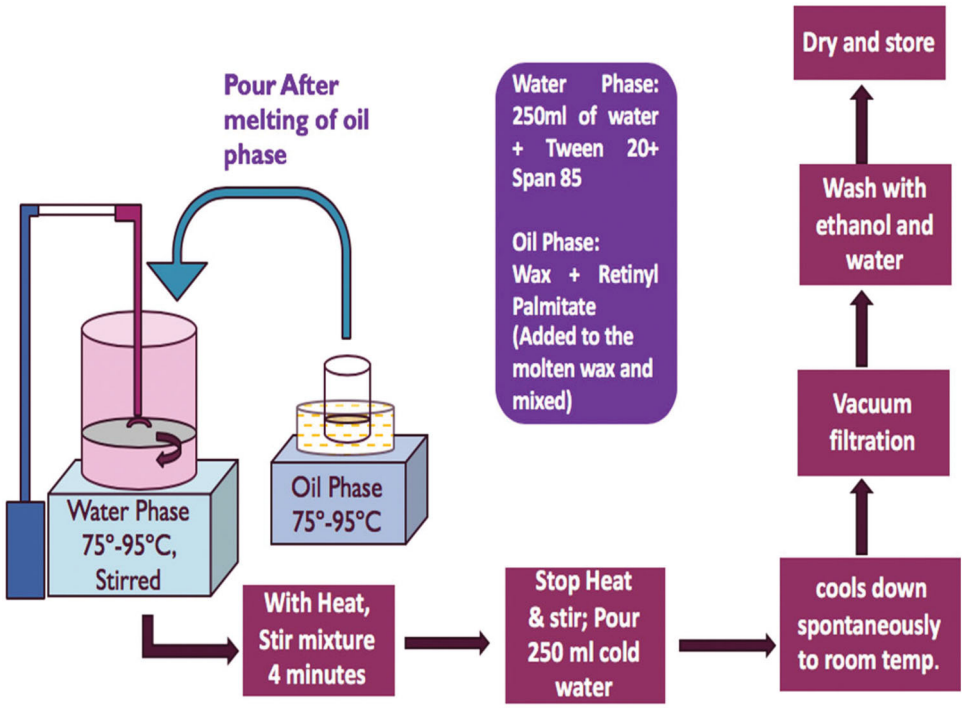


**Figure 2.** Schematic of microencapsulation by melt dispersion- an oil-in-water method, where the oil phase consisting of retinyl palmitate and melted wax were poured and dispersed into the water phase i.e. an emulsion mixture consisting of DI water and surfactants through mechanical stirring. Subsequent pouring of ice-cold water enabled solidification of wax droplets, resulting in free-flowing particles upon filtration and drying.

For measuring how much of emulsifier (A) to blend with emulsifier (B) value of *X* (w/w), Equations (1) and (2) were used.

$$\%A = \frac{(X - HLBb) \times 100}{HLBa - HLBb} \quad (1)$$

$$\%B = 100\% - \%A \quad (2)$$

where: X = desired HLB value (For Beeswax and Paraffin wax, 10 and Carnauba wax, 12), A = Tween 20, B = Span 85, $HLB_a$ = HLB of Tween 20, $HLB_b$= HLB of Span 85.

## Statistical analysis of the effect of process variables on microcapsule properties

A three-level definitive screening design was applied to assess the effect of four important factors: type of wax, theoretical loading capacity, emulsifier concentration, and stirring speed. The response variables we looked into were the actual loading capacity% (w/w), encapsulation efficiency (%), antioxidant activity (%), and mean size of produced microcapsules. We conducted nine experiments based on the design of experiment, as mentioned in Table 1.

We used three types of wax, namely beeswax, paraffin wax, and carnauba wax to compare their performance as a shell material.

As the loading of the active compound in the mixture is an important factor that influences the characteristics of the particles, we investigated three levels of the theoretical loading capacity in this study: 10%, 15%, and 25%. We did not choose a higher level because a higher loading percentage could compromise the wall barrier as well as the stability of the microcapsules. As a response variable, encapsulation efficiency of more than 50% was considered to be acceptable that can enable upscaling (Gavory *et al.* 2014).

The levels chosen for evaluating the effect of surfactant percentage were 0%, 1%, and 2%, in order to compare the morphology of particle produced with no surfactant and gradually with higher ratios of surfactant. The levels of stirring speed were chosen to be 180, 230 and 280 rpm.

We fitted an Analysis of Variance (ANOVA) model to analyse the data, with wax-type as a qualitative factor and others as quantitative factors, where actual levels of factors were used. Their significance was tested with *F*-test..

## Characterisation

*Differential Scanning Calorimetry (DSC) analysis:* DSC of the waxes were carried out by using Mettler Toledo DSC821e instrument, where a standard empty

**Table 1.** Design of experiment with four factors (type of wax, theoretical loading% (w/w), surfactant% (w/v) and stirring speed) at three levels: −1,0,1 (specified in the table).

| Experiment | A | B | C | D | Factors | Levels |
|---|---|---|---|---|---|---|
| 1 | 1 | 0 | 1 | −1 | A = Type of wax | For A: |
| 2 | 0 | −1 | 1 | 1 | B = Theoretical Loading (%) | 1 = Beeswax, 0= Paraffin, |
| 3 | 0 | 1 | −1 | −1 | C = Surfactant (%) | −1= Carnauba |
| 4 | −1 | 0 | −1 | 1 | D = Speed (rpm) | For B: |
| 5 | 0 | 0 | 0 | 0 | | 1 = 25%, 0 = 15%, −1 = 10 |
| 6 | −1 | 1 | 1 | 0 | | For C: |
| 7 | 1 | 1 | 0 | 1 | | 1 = 2%, 0 = 1%, −1 = 0% |
| 8 | −1 | −1 | 0 | −1 | | For D: |
| 9 | 1 | −1 | −1 | 0 | | 1 = 280, 0 = 230, −1 = 180 |

aluminium pan was used as the reference. Samples were scanned from 25 °C to 100 °C under $N_2$ atmosphere with a heating rate of 10 °C/min, and then reversely cooled at the rate of −10 °C/min from 100 °C to 25 °C. All samples were prepared with weights between 2.0 and 10.0 mg.

*Thermogravimetric analysis (TGA):* In order to understand the stability of microcapsule in during storage and transportation, thermal stability of the three waxes were assessed with TA Instruments Discovery TGA-MS by scanning the samples from 25 °C to 600 °C under $N_2$ atmosphere at a heating rate of 10 °C/min. Samples were prepared with weights between 12.0 and 25 mg.

*Size and Morphology:* We observed the shape, morphology, and size distribution of the produced microcapsules by using FE-SEM FEI Teneo scanning electron microscope and Image-J 1.51 s digital image analyser. Samples were vacuum coated with a gold film after mounting them on copper stubs and then surface morphology was examined using an FEI Teneo SEM.

*Loading Capacity and Encapsulation Efficiency:* We characterised the particles based on loading capacity and encapsulation efficiency. Loading capacity was defined as the ratio of the weight of RP to the weight of total encapsulation material for shell and core, expressed in percentage. Expected loading capacity was calculated by taking into account the amount of RP initially used for production. Actual loading capacity provided the actual amount of RP loaded, excluding the amount lost during the process due to evaporation as well as solidification with wax in the container wall. Encapsulation efficiency was defined as the ratio of actual loading capacity to expected loading capacity, expressed in percentage. Hence, these terms can be expressed by Equations (3)–(5):

$$\text{Expected LC\%} = \frac{M_0}{M_0 + M_p} \times 100 \quad (3)$$

$$\text{Actual LC\%} = \frac{M_e}{M_e + M_p} \times 100 \quad (4)$$

$$\text{EE\%} = \frac{\text{Actual LC\%}}{\text{Expected LC}} \times 100 \quad (5)$$

where, $M_0$ = initial weight of Vitamin A; $M_e$ = weight of Vitamin A encapsulated, $M_p$ = amount of wall material used.

Pure ethanol containing a fixed amount of microparticles was heated to the boiling temperature of wax for 15 min to release all the content of the capsules. Then the system was stirred for 1 hr without heat. The extractant was filtered using the syringe, and the volume was recorded. All samples were measured in triplicates. The supernatant was diluted with ethanol to an appropriate concentration. The diluted solution for each sample was replaced in quartz cuvette containing ethanol in each respective test to achieve UV-Vis (Ultraviolet-visible spectroscopy) absorbance spectrum. The concentration was determined by using the absorbance at 327 nm and a concentration curve of known concentrations of the RP.

*Antioxidant activity (DPPH assay):* Evaluation of antioxidant activity was carried out by assay of 2,2-diphenyl-1-picrylhydrazyl (DPPH) free radical scavenging activity, DPPH is a stable free radical that becomes a stable diamagnetic molecule by accepting an electron or hydrogen radical. As a result, a decrease in absorbance at 517 nm should be observed.

In our experiments, 100 µl of sample or control (ethanol) was added to 3.9 ml of DPPH solution (ethanol; 60 µM, 25 mg/L). We measured absorbance at 517 nm, using UV spectrophotometer at the time after 1 hr of shaking in the dark. We used the following equation to determine Antioxidant activity (AA %):

$$AA\% = \frac{A_0 - A_1}{A_0} \times 100 \quad (6)$$

Where: $A_0$ is the blank (contains only ethanol), and $A_1$ is the sample.

## Results and discussion

### Thermal properties of waxes

Study of the thermal properties of waxes using DSC verifies the melting and crystallization temperature of the waxes, which helped to decide the processing temperature during the preparation and characterisation of microcapsules. TGA evaluated the thermal decomposition of waxes in order to compare the thermal stability of the three waxes. Besides, the thermal stability of the waxes allows us to understand conditions for the storage and transportation of cosmetic products.

Beeswax is an insect wax secreted from honeybees, consisting mainly of fatty acid esters (65%), hydrocarbons (23%), free acids (12%) and free alcohols (1%) (Tulloch 1970). In the DSC curve (Figure 3.1), beeswax showed its melting peak ($T_m$) around 65.84 °C and crystallization peak ($T_c$) at around 57.5 °C. Paraffin wax, being derived from petroleum source and composed of mostly hydrocarbons (Himran *et al.* 1994), showed $T_m$ at around 64.73 °C and $T_c$ at around 54.83 °C, which were lower than the $T_m$ and $T_c$ of beeswax, respectively. Carnauba wax is a hard wax derived from Brazilian palm leaves, usually with a high content of aliphatic esters (38–40%), diesters of fatty acids (30–34%), a small number of fatty alcohols (10–12%), acids, hydrocarbons, etc. (Vandenburg and Wilder 1970). The $T_m$ of carnauba wax was found at 87 °C whereas the $T_c$ was at 77 °C. Therefore, carnauba wax exhibited the highest melting and crystallization temperatures. These results were consistent with the results obtained by Ruguo *et al.* (2011) for the thermal properties of the three waxes.

From the TGA and DTG (first derivative of TG) curves (Figure 3.2), the beeswax sample showed initial decomposition around 312 °C, and after 465 °C, the sample completely decomposed. The highest rate of decomposition was around 375 °C. Similarly, the onset of decomposition of paraffin wax was at 265 °C and the highest rate of decomposition at 318 °C. For carnauba wax, the onset of decomposition was at 381 °C, while the highest rate of decomposition was at 426 °C. Therefore, among the three waxes, carnauba wax was found to be the most thermally stable, whereas paraffin wax had the least thermal stability.

Turton and Cheng (2007) reported that the stable temperature for incorporating active substances into melt-solidified matrices should be in the range of 30 °C − 200 °C and the range of melting temperature should be narrow. All results obtained from DSC and TGA for the melting temperature and thermal stability comply with these requirements.

### Effect of process variables on microcapsule properties

For the four response variables: actual loading capacity, encapsulation efficiency, antioxidant activity, and mean particle size, the results of nine experiments are reported in Table 2.

### Loading capacity and encapsulation efficiency

We scanned the supernatant of extracted microcapsules with UV-Vis spectrophotometry from 190 nm to 1100 nm. For both beeswax and carnauba wax as shell materials, the wavelength of maximum absorbance, $\lambda_{max}$ was observed approximately at 327 nm, which is the peak wavelength for RP (Figure 4). Therefore, it became evident that RP remained stable throughout the production and extraction process, and no other species were formed in the process.

Gangurde and Amin (2017) prepared Vitamin A palmitate microcapsules for topical drug delivery, using combination of maltodextrin and modified starches as shell materials by spray drying method. Their encapsulation efficiency ranged from 53% to 63%. In our study, the encapsulation efficiency was more than 60% for all of the experiments. The highest encapsulation efficiency achieved was 91% for paraffin wax, with actual theoretical loading capacity 15%, surfactant 1% and stirring speed of 230 rpm. Statistically, the efficiency was not affected by the type of wax, theoretical loading%, surfactant%, and stirring speed. However, the actual loading capacity was significantly affected by the theoretical loading capacity, as expected ($p$ values $= 0.00232$, significance level, $\alpha = 1\%$). Following statistical model was obtained:

$$\text{Actual loading} = -2.7 + 0.7\ \text{Theoretical loading};$$

$$R^2 = 0.97$$

Therefore, it can be predicted that for one unit increase in theoretical loading (%), the actual loading will increase by 0.7%. The $R^2$ value of this model is 0.97, that means 97% of the variance in actual loading capacity (%) can be explained by the theoretical loading (%).

Within an optimum level of theoretical loading capacity, the active oil phase can be entrapped within the molten wax matrix to form microcapsules. Conversely, at a much higher level of theoretical loading, the amount of wall material would not be sufficient to

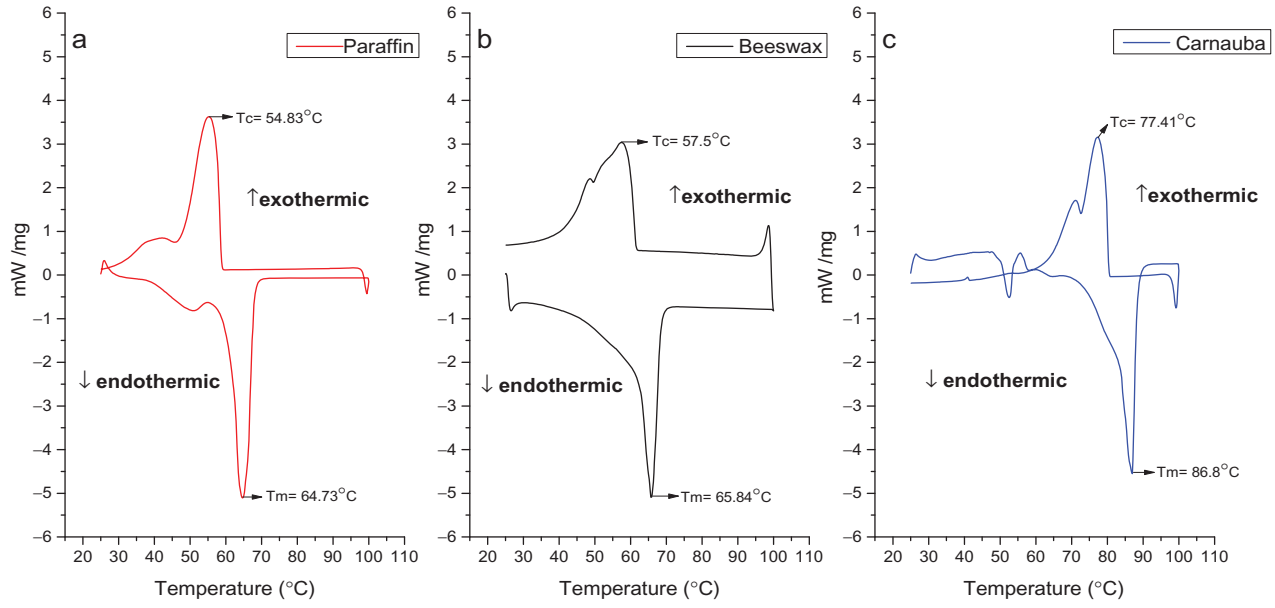


**(3.1)**

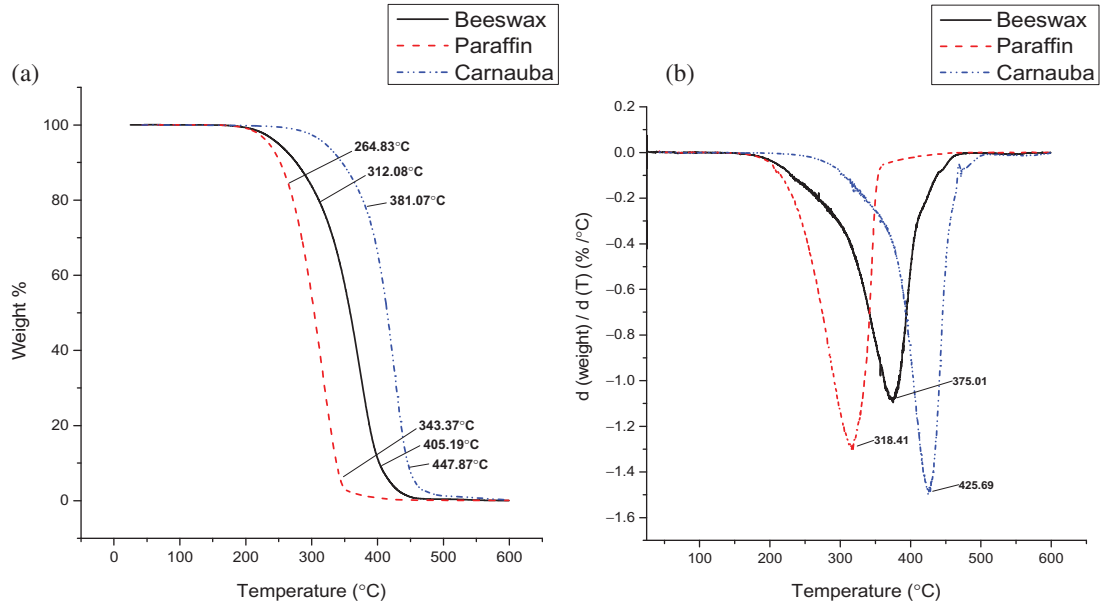


**(3.2)**

**Figure 3.** Thermal characterisation of three waxes. (3.1) DSC of (a) paraffin wax (b) beeswax and (c) carnauba wax (scanned from 25 °C to 100 °C under $N_2$ atmosphere with a heating rate of 10 °C/min) show their melting peaks and crystallization peaks. (3.2) (a) TGA and (b) DTG of beeswax, paraffin wax & carnauba wax (scanned from 25 °C to 600 °C under $N_2$ atmosphere at a heating rate of 10 °C/min) show the thermal decomposition of the waxes.

encapsulate the core material, hence would practically result in unstable particles with poor actual loading. Barakat and Yassin (2006) attempted a theoretical loading of 50% to encapsulate carbamazepine using molten Precifac® ATO 5 (PRF), which led to aggregated and fragile particles, making them unsuitable for drug delivery.

### *Antioxidant activity (DPPH assay)*

In all of the experiments, the particles showed antioxidant activity. The mean antioxidant activity ranged from 4% to 20%. The results of antioxidant activity varied in each experiment without a definite pattern; therefore, statistically, none of the process variables came out to be significant ($p > 0.1$). This

**Table 2.** Results of nine experiments for four process parameter (type of wax, theoretical loading, surfactant% and stirring speed) at three levels on four response variables: mean actual loading capacity% ($n = 3$), mean encapsulation efficiency% ($n = 3$), mean antioxidant activity ($n = 3$), and mean size ($n = 30$, except for experiment 3, $n = 8$).

| | Process variables | | | | Response variables | | | |
|---|---|---|---|---|---|---|---|---|
| Experi-ments | A Type of wax | B Theoretical loading (% w/w) | C Surfactant (% w/v) | D Stirring speed (rpm) | Mean actual LC ± SD (% w/w) $n = 3$ | Mean EE ± SD (%) $n = 3$ | Mean AA ± SD (%) $n = 3$ | Mean size ± SD (μm) span = (D90–D10)/D50 |
| 1 | 1 | 0 | 1 | −1 | 11.01 ± 0.45 | 73.40 ± 2.98 | 6.36 ± 0.61 | 94 ± 43 *n = 30, span = 1.43* |
| 2 | 0 | −1 | 1 | 1 | 7.65 ± 0.39 | 76.60 ± 3.95 | 5.9 ± 1.00 | 69 ± 31 *n = 30, span = 1.14* |
| 3 | 0 | 1 | −1 | −1 | 17.33 ± 1.25 | 69.26 ± 5 | 20.39 ± 0.64 | 464 ± 318 *n = 8, span = 2.13* |
| 4 | −1 | 0 | −1 | 1 | 12.34 ± 0.94 | 82.17 ± 6.27 | 5.17 ± 0.88 | 213 ± 167 *n = 30, span = 2.16* |
| 5 | 0 | 0 | 0 | 0 | 12.13 ± 1.54 | 80.77 ± 10.26 | 4.1 ± 2.44 | 124 ± 44 *n = 30, span = 1.03* |
| 6 | −1 | 1 | 1 | 0 | 17.63 ± 0.78 | 70.52 ± 3.14 | 6.27 ± 1.63 | 28 ± 20 *n = 30, span = 2.33* |
| 7 | 1 | 1 | 0 | 1 | 19.8 ± 1.18 | 79.22 ± 4.7 | 10.70 ± 1.25 | 86 ± 42 *n = 30, span = 1.28* |
| 8 | −1 | −1 | 0 | −1 | 7.79 ± 0.16 | 77.53 ± 1.81 | 15.8 ± 3.19 | 36 ± 24 *n = 30, span = 2.69* |
| 9 | 1 | −1 | −1 | 0 | 6.06 ± 0.18 | 60.18 ± 1.76 | 10.49 ± 3.26 | 162 ± 124 *n = 30, span = 2.48* |

LC: Loading capacity; EE: Encapsulation efficiency; AA: Antioxidant activity; SD: Standard deviation.
For A: 1 = Beeswax, 0 = Paraffin, −1 = Carnauba; For B: 1 = 25%, 0 = 15%, −1 = 10; For C: 1 = 2%, 0 = 1%, −1 = 0%; For D: 1 = 280, 0 = 230, −1 = 180. Span values of particle size distribution shown are calculated by the equation, span= (D90–D10)/D50, where D90, D10, and D50 correspond to the 90%, 10% and 50% point of diameter respectively.

result was surprising because theoretical loading% and encapsulation efficiency (affecting the concentration of active ingredient) should have effects on the antioxidant activity. Moreover, RP was found to be stable in the prepared microcapsules (Figure 4). The highest antioxidant activity of 20% was observed for experiment 3, where 25% RP was loaded into paraffin wax, with no surfactant and minimum speed level of 180 rpm. This experiment resulted in agglomerated mass instead of particles with an encapsulation efficiency of 69%, so the high antioxidant activity could be due to the large amount of protective shell in the mass. On the contrary, lowest antioxidant activity of 4% was observed for microcapsules produced with paraffin wax, with 15% theoretical loading, 1% surfactant and 230 rpm stirring speed. This result was also unlikely as the encapsulation efficiency was around 81%. Hence, the effect of the process parameters on antioxidant activity was considered inconclusive. The most probable reason is that the assay of DPPH free radical scavenging was affected by solvent interactions and very low concentration of RP in the supernatant, leading to inconsistent reading in the ultraviolet-visible spectroscopy. Further research needs to be completed in order to develop a more suitable method and understand how the antioxidant activity is affected throughout the process of production and extraction.

### *Size and morphology*

The morphology, size, distribution and shape of the microcapsules produced with varying process parameters were analysed from the SEM images of the particles.

Type of wax did not have a significant effect on the response variables ($p > 0.1$), despite the differences in their chemical composition. However, particles with carnauba wax as shell material appeared to have smoother surface morphology (Figure 5.2) compared to those with beeswax and paraffin wax.

The particles produced without any surfactant, irrespective of other factors, did not possess a definite size and shape and they often coalesced into large mass (Figure 5.1(c), 5.1(d), 5.1(i) and 5.2(c), 5.2(d), 5.2(i)). Consequently, the mean size for such particles was more than 160 μm. (Table 2). A similar result was found in a study with ibuprofen drug microparticles encapsulated in carnauba wax with no surfactants. (Bodmeier *et al.* 1992). On the other hand, with the presence of surfactant, all of the rest of the experiments could produce particles with spherical shape and small size in micron scale. The reason behind this phenomenon is the role of surfactant in the lowering

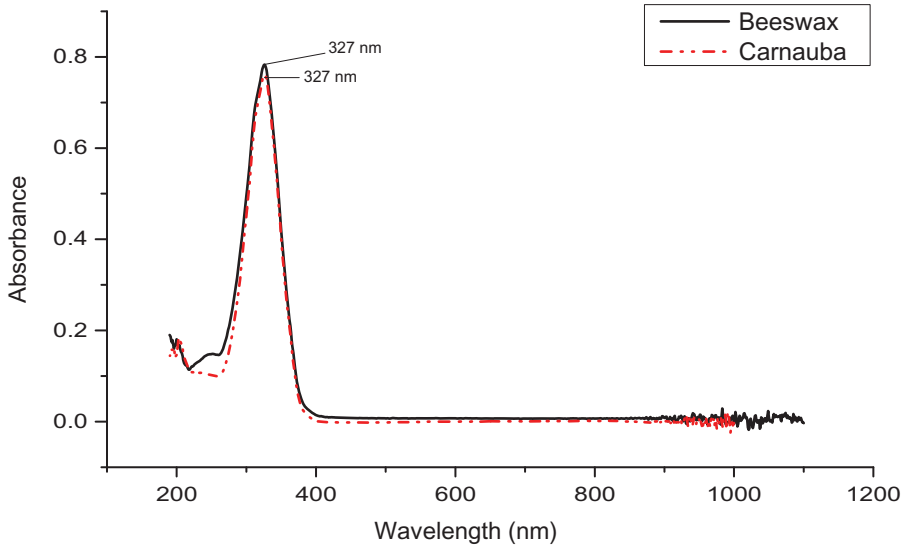


**Figure 4.** Ultra violate-visible spectrophotometry of supernatant of extracted microcapsules (scanned from 190 nm to 1100 nm) showed maximum absorbance at 327 nm i.e. the peak wavelength of retinyl palmitate (RP), thus confirmed stability of RP during the preparation and extraction of microcapsules.

of interfacial tension and the partition of particles. The presence of surfactants induces a repulsive force among the droplets, hence prevents their agglomeration and promotes stabilisation. The surface of the microcapsules appeared to be rough and porous, which might contribute to the leaching of the core over time. In the statistical analysis, it was found that the amount of surfactant significantly affects the size of microcapsules ($p = 0.0573$, $\alpha = 10\%$), supporting the result from image analysis. This result is similar to another study (Ahlin *et al.* 1998), where solid lipid nanoparticles were prepared by the melt-emulsification process, and optimum surfactant concentration was found to be around 2–3%.

From our applied statistical model, following relationship was obtained:

$$\text{Mean size} = 249.5 - 107.9\ \text{Surfactant},\ R^2 = 0.48$$

Therefore, it can be predicted that for one unit increase in surfactant (%), the mean size of particles will decrease by 107.9 μm. The $R^2$ value denotes that 48% of the variance in mean size can be predicted from the amount of surfactant (%). Here $R^2$ is not high, which is consistent with the fact that the regression coefficient corresponding to surfactant is significant only at level alpha = 10% but not at 5%. The reason for this is due to the large mean and standard deviation of size observed for experiment 3, 4 and 9. In the absence of surfactant, the agglomerated mass was produced instead of free-flowing particles. As a result, this value acted as an outlier and affected the overall correlation between surfactant (%) and mean size.

Microcapsules can be classified into three types according to the basic morphology of how the core material is distributed within the system: mononuclear, polynuclear, and matrix form (Mishra 2016), as illustrated in Figure 6.1. A mononuclear or core-shell type has a single core with a shell around it. Polynuclear capsules have multiple cores within the shell. Matrix capsules have their core material homogeneously or heterogeneously distributed throughout or within the shell material. Particles produced through melt dispersion of waxes mostly produce non-homogeneous, matrix microcapsules, however, may also consist of hollow-shell morphology (Djordjević *et al.* 2015). From the electron microscopy of cut microcapsules (prepared with beeswax shell, 10% loading capacity, 0% surfactant and 230 rpm), we found evidence that the microcapsules have typical hollow-shell as well as matrix morphology (Figure 6.2). Therefore the core retinyl palmitate is distributed within the shell.

The particle size distributions indicate that the produced particles are mostly inhomogeneous and non-uniform in size, which is evident with the high standard deviation of the mean size of particles (Table 2). Djordjević *et al.* (2015) described the size of particles prepared by melt dispersion as non-uniform, corroborating with our results for most of the experiments.

The speed levels (180, 230 and 280 rpm) chosen were within the range of a simple laboratory mechanical mixer. Previous studies (Barakat and Yassin 2006, Gowda and Shivakumar 2007, Milanovic *et al.* 2011)

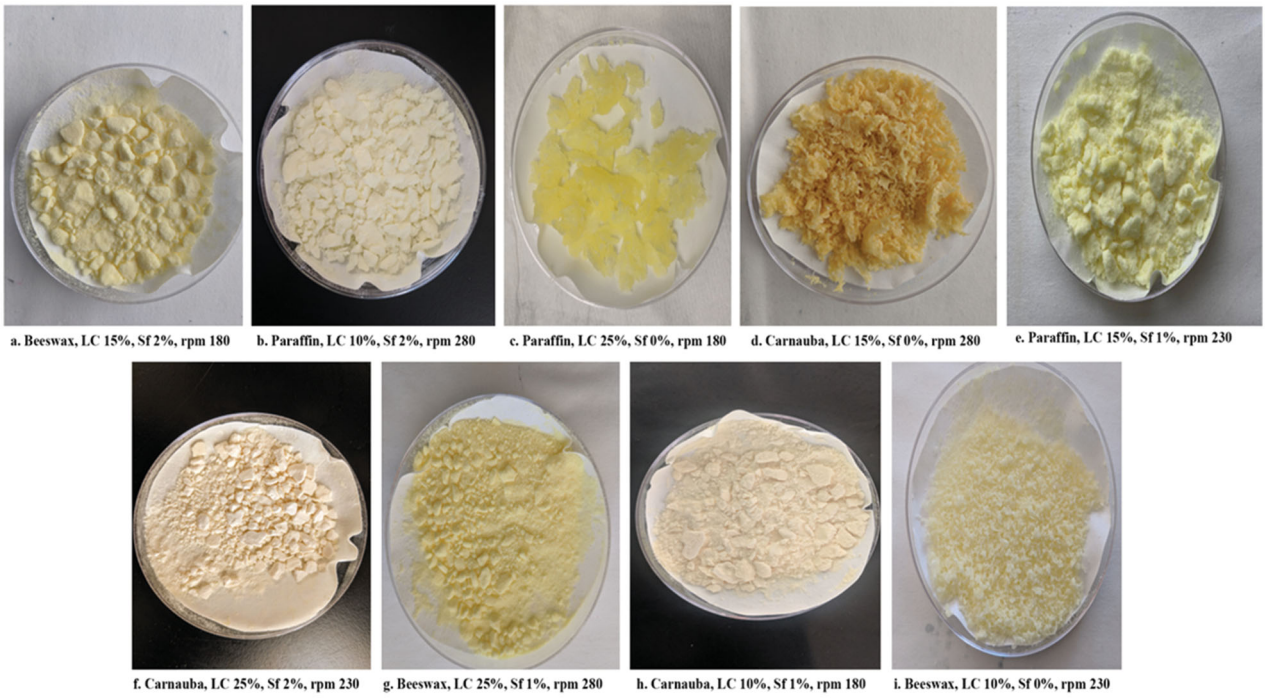


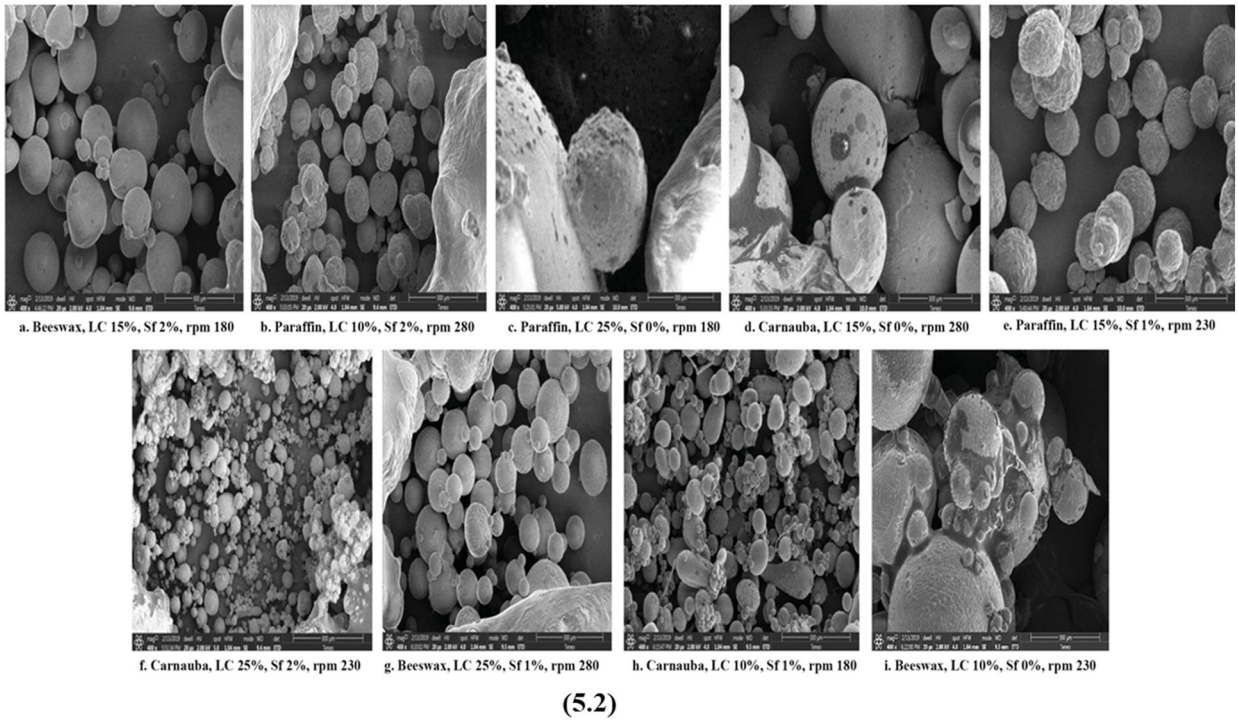


**Figure 5.** Surface morphology of microcapsules- (5.1) photographs of microcapsules (5.2) Scanning electron microscopy (SEM) images of microcapsules (400× magnification) prepared according to design of experiment: (a) Beeswax, LC 15%, Sf 2%, rpm 180 (b) Paraffin, LC 10%, Sf 2%, rpm 280 (c) Paraffin, LC 25%, Sf 0%, rpm 180 (d) Carnauba, LC 15%, Sf 0%, rpm 280 (e) Paraffin, LC 15%, Sf 1%, rpm 230 (f) Carnauba, LC 25%, Sf 2%, rpm 230 (g) Beeswax, LC 25%, Sf 1%, rpm 280 (h) Carnauba, LC 10%, Sf 1%, rpm 180 (i) Beeswax, LC 10%, Sf 0% rpm 230.

on such process parameters investigated the effect of stirring speed on particle size at a much higher range (∼1000 rpm). We studied a lower range of stirring speed in order to compare their effectiveness and estimate optimum speed level for successful encapsulation with much less consumption of energy.

Stirring speed (within low-speed range ∼300 rpm) showed no significant effect on the responses,

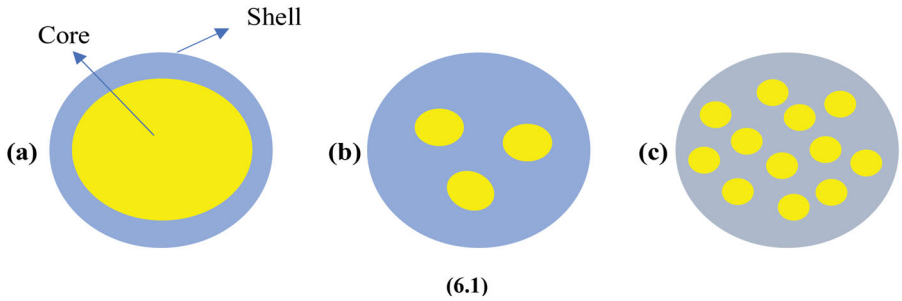


(6.1)

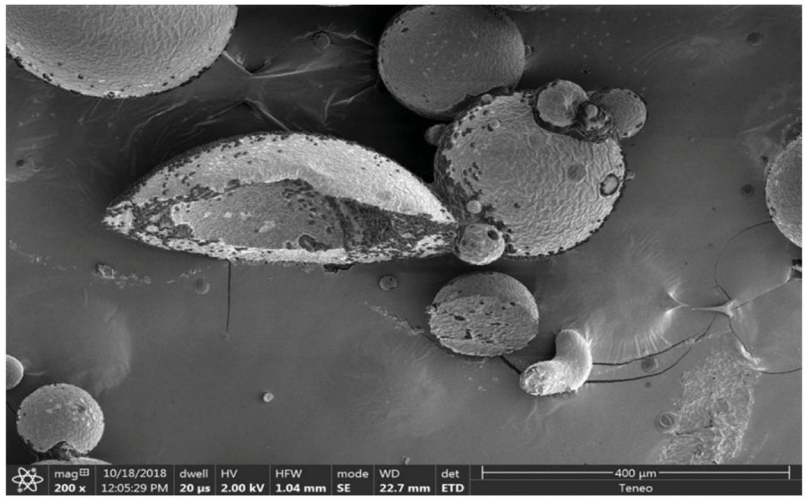


(6.2)

**Figure 6.** Morphology of microcapsules: (6.1) Types of microcapsules according to morphology- (a) mononuclear (b) polynuclear (c) matrix (6.2) SEM image (200× magnification) of cut RP-loaded beeswax microcapsules (prepared with beeswax shell, 10% loading capacity, 0% surfactant and 230 rpm) showing both hollow shell-core and matrix morphology.

including the size of particles ($p > 0.1$). This result is unusual according to existing literature, specifically because higher speed should impart more shear force to break droplets in the emulsion, resulting in smaller particles. Barakat and Yassin (2006) found a gradual decrease in average size when stirring speed was elevated from 400 rpm to 800 rpm. A similar result was found for a speed range of 900–100 rpm by Gowda and Shivakumar (2007) and 1000–1500 rpm by Milanovic *et al.* (2011). However, a plausible explanation for the outcome in our study can be that due to the low range of the levels of speed, the interaction with high surfactant concentration could overcome the limitation of low speed (such as 180 rpm). On the contrary, a comparatively higher speed (such as 280 rpm), being still in the low-speed range (<300 rpm), could not overcome the effect of zero surfactant concentration, that is, a high interfacial force. Hence, it can be concluded that with appropriate surfactant concentration, it is possible to attain good efficiency (>70%) with a mean particle size as small as 35 µm even at the low speed level. Hence, the highest speed level chosen in this study i.e. 280 rpm can be used along with high surfactant% (2%) to develop small microparticles.

Through statistical analysis, theoretical loading capacity and surfactant% came out to be prominent factors affecting the actual loading capacity and mean size of particles, respectively. Although type of wax did not significantly affect the results, beeswax provides the best feasibility among the three waxes due to low melting temperature, flexibility, eco-friendliness and natural skin healing properties. Therefore, an optimal formula for preparing microcapsules with high loading capacity and small mean size can be 25% theoretical loading, 2% surfactant and stirring speed 280 rpm, using beeswax as the shell material.

## Conclusion

This study demonstrated that RP can be successfully encapsulated in a wax matrix by using the melt-dispersion method. Encapsulation efficiency of around 60 − 80% was achieved, where mean particle size had high variation, ranging around 30 µm–500 µm. The statistical analysis revealed that theoretical loading

and surfactant% can play significant roles in controlling the actual loading, and size of the capsules, based on the intended application such as cosmetic exfoliating scrubs, facial wipes, etc. Thus this research makes a foundation to develop cost-effective, organic and eco-friendly innovative cosmeceuticals as well as cosmetotextiles containing retinoids. In the future study, the shelf life, kinetic release mechanism and application of the prepared microcapsules in cosmetic formulations and textile substrates will be evaluated.

## Disclosure statement

No potential conflict of interest was reported by the author(s).

## Funding

This work was supported by AATCC Foundation Student Research Support Grant 2019.

## References

360 Research Reports. 2018. Global cosmeceuticals market - segmented by product type, active ingredients, and region - growth, trends, and forecasts (2018 - 2023) [Online]. Available from: https://www.360researchreports.com/global-cosmeceuticals-market-13101678 .

Ahlin, P., Kristl, J., and Smid-Korbar, J., 1998. Optimization of procedure parameters and physical stability of solid lipid nanoparticles in dispersions. *Acta pharmaceutica*, 48, 259–267.

Banjare, L., and Ghillare, N., 2012. Development of biocompatible nanoparticles for sustained topical delivery of Rutin. *International journal of pharmaceutical and biological archives*, 3, 326–332.

Barakat, N.S., and Yassin, A.E.B., 2006. In vitro characterization of carbamazepine-loaded precifac lipospheres. *Drug delivery*, 13 (2), 95–104.

Barroso, M.R., *et al.*, 2014. Exploring the antioxidant potential of *Helichrysum stoechas* (L.) Moench phenolic compounds for cosmetic applications: chemical characterization, microencapsulation and incorporation into a moisturizer. *Industrial crops and products*, 53, 330–336.

Benita, S., 2005. *Microencapsulation: methods and industrial applications.* New York: CRC Press.

Bhalerao, S., and Raje Harshal, A., 2003. Preparation, optimization, characterization, and stability studies of salicylic acid liposomes. *Drug development and industrial pharmacy*, 29 (4), 451–467.

Bodmeier, R., Wang, J., and Bhagwatwar, H., 1992. Process and formulation variables in the preparation of wax microparticles by a melt dispersion technique. I. Oil-in-water technique for water-insoluble drugs. *Journal of microencapsulation*, 9 (1), 89–98.

Boerman, M.H., and Napoli, J.L., 1996. Cellular retinol-binding protein-supported retinoic acid synthesis relative roles of microsomes and cytosol. *Journal of biological chemistry*, 271 (10), 5610–5616.

Bradley, E.J., *et al.*, 2015. Over-the-counter anti-ageing topical agents and their ability to protect and repair photoaged skin. *Maturitas*, 80 (3), 265–272.

Casanova, F., and Santos, L., 2016. Encapsulation of cosmetic active ingredients for topical application–a review. *Journal of microencapsulation*, 33 (1), 1–17.

Counts, D.F., Skreko, F., and Mcbee, J., 1988. The effect of retinyl palmitate on skin composition and morphometry. *Journal of the society of cosmetic chemists*, 39, 235–240.

Davies, J. 1957. A quantitative kinetic theory of emulsion type. I. Physical chemistry of the emulsifying agent. Gas/Liquid and Liquid/Liquid Interface. *In:* Proceedings of the international congress of surface activity. London: Butterworths, 426–438.

Deshmukh, R., Wagh, P., and Naik, J., 2016. Solvent evaporation and spray drying technique for micro-and nanospheres/particles preparation: a review. *Drying technology*, 34 (15), 1758–1772.

Djordjević, V., *et al.*, 2015. *Melt-dispersion technique for encapsulation. Handbook of encapsulation and controlled release*. Boca Raton: CRC Press.

Duclairoir, C., *et al.*, 2002. α-Tocopherol encapsulation and in vitro release from wheat gliadin nanoparticles. *Journal of microencapsulation*, 19 (1), 53–60.

Duell, E.A., Kang, S., and Voorhees, J.J., 1997. Unoccluded retinol penetrates human skin in vivo more effectively than unoccluded retinyl palmitate or retinoic acid. *The journal of investigative dermatology*, 109 (3), 301–305.

Fisher, G.J., *et al.*, 1999. Molecular mechanisms of photoaging in human skin in vivo and their prevention by all-trans retinoic acid. *Photochemistry and photobiology*, 69 (2), 154–157.

Fisher, G.J., and Voorhees, J.J., 1998. Molecular mechanisms of photoaging and its prevention by retinoic acid: ultraviolet irradiation induces MAP kinase signal transduction cascades that induce Ap-1-regulated matrix metalloproteinases that degrade human skin in vivo. *Journal of investigative dermatology symposium proceedings*, 3, 61–68.

Ganceviciene, R., *et al.*, 2012. Skin anti-aging strategies. *Dermato-endocrinology*, 4 (3), 308–319.

Gangurde, A.B., and Amin, P.D., 2017. Microencapsulation by spray drying of vitamin A palmitate from oil to powder and its application in topical delivery system. *Journal of encapsulation and adsorption sciences*, 07 (01), 10–39.

Gavory, C., *et al.*, 2014. Encapsulation of a pressure sensitive adhesive by spray-cooling: optimum formulation and processing conditions. *Advanced powder technology*, 25 (1), 292–300.

Giri, T.K., *et al.*, 2013. Prospects of pharmaceuticals and biopharmaceuticals loaded microparticles prepared by double emulsion technique for controlled delivery. *Saudi pharmaceutical journal*, 21, 125–141.

Goncalves, A., Estevinho, B.N., and Rocha, F., 2016. Microencapsulation of vitamin A: a review. *Trends in food science & technology*, 51, 76–87.

Gowda, D., and Shivakumar, H., 2007. Preparation and evaluation of waxes/fat microspheres loaded with lithium carbonate for controlled release. *Indian journal of pharmaceutical sciences*, 69 (2), 251.

Griffin, W.C., 1949. Classification of surface-active agents by HLB. *Journal of the society of cosmetic chemists*, 1, 311–326.

Harris, R., *et al.*, 2011. Chitosan nanoparticles and microspheres for the encapsulation of natural antioxidants extracted from Ilex paraguariensis. *Carbohydrate polymers*, 84 (2), 803–806.

Himran, S., Suwono, A., and Mansoori, G.A., 1994. Characterization of alkanes and paraffin waxes for application as phase change energy storage medium. *Energy sources*, 16 (1), 117–128.

Irani, F., *et al.*, 2019. Fabrication and characterization of microencapsulated n-heptadecane with graphene/starch composite shell for thermal energy storage. *Progress in organic coatings*, 131, 203–210.

Irani, F., *et al.*, 2017. Microencapsulation of n-heptadecane phase change material with starch shell. *Progress in organic coatings*, 113, 31–38.

Ito, F., *et al.*, 2013. Possibility for the development of cosmetics with PLGA nanospheres. *Drug development and industrial pharmacy*, 39 (5), 752–761.

Jenning, V., *et al.*, 2000. Vitamin A loaded solid lipid nanoparticles for topical use: occlusive properties and drug targeting to the upper skin. *European journal of pharmaceutics and biopharmaceutics*, 49 (3), 211–218.

Jimtaisong, A., and Saewan, N., 2014. Utilization of carboxymethyl chitosan in cosmetics. *International journal of cosmetic science*, 36 (1), 12–21.

Jones, B., and Nachtsheim, C.J., 2011. A class of three-level designs for definitive screening in the presence of second-order effects. *Journal of quality technology*, 43 (1), 1–15.

Jyothi, S.S., *et al.*, 2012. Microencapsulation: a review. *International journal of pharma and bio sciences*, 3, 509–531.

Kim, D.-G., *et al.*, 2006. Retinol-encapsulated low molecular water-soluble chitosan nanoparticles. *International journal of pharmaceutics*, 319 (1–2), 130–138.

Kim, H.J., *et al.*, 2010. Microencapsulation of rosmarinic acid using polycaprolactone and various surfactants. *International journal of cosmetic science*, 32 (3), 185–191.

Koo, B.M., *et al.*, 2008. Encapsulation and stabilization of photo-sensitive antioxidants by using polymer microcapsules with controlled phase heterogeneity. *Macromolecular rapid communications*, 29 (6), 498–502.

Lee, M.-H., *et al.*, 2001. Preparation of silica particles encapsulating retinol using O/W/O multiple emulsions. *Journal of colloid and interface science*, 240 (1), 83–89.

Lupo, M.P., 2001. Antioxidants and vitamins in cosmetics. *Clinics in dermatology*, 19 (4), 467–473.

Martins, I.M., *et al.*, 2009. Microencapsulation of thyme oil by coacervation. *Journal of microencapsulation*, 26 (8), 667–675.

Mccall, R.L., and Sirianni, R.W., 2013. PLGA nanoparticles formed by single-or double-emulsion with vitamin E-TPGS. *Journal of visualized experiments*, (82), p.e51015.

Milanovic, J., *et al.*, 2011. Carnauba wax microparticles produced by melt dispersion technique. *Chemical papers*, 65 (2), 213–220.

Mishra, M., 2016. *Handbook of encapsulation and controlled release*. Boca Raton: CRC press.

Mokhatab, S., Poe, W. A., and Mak, J. Y., 2018. *Handbook of natural gas transmission and processing: principles and practices.* Cambridge: Gulf Professional Publishing.

MORICE, C.-H. 2016. *Choosing the right PE beads alternative* [Online]. Available: https://www.in-cosmetics.com/RXUK/RXUK_InCosmetics/2016-website/Innovation%20Seminar%20Presentations/Presentation_Lessonia_Innovation%20seminar.pdf?v=635974319593299169 [Accessed July 18 2019].

Oliveira, M.B., *et al.*, 2014. Topical application of retinyl palmitate-loaded nanotechnology-based drug delivery systems for the treatment of skin aging. *BioMed research international*, 2014, 632570.

Ömeroğullari BaşyiĞi, Z., *et al.*, 2018. Vitamin E loaded fabrics as cosmetotextile products: formulation and characterization. *Journal of textile & apparel/tekstil ve konfeksiyon*, 28 (2).

Ruguo, Z., *et al.*, 2011. Thermal analysis of four insect waxes based on differential scanning calorimetry (DSC). *Procedia engineering*, 18, 101–106.

Saini, H., and Manideep, K., 2017. Cosmetotextiles: a novel technique of developing wearable skin care. *Asian journal of home science*, 12, 289–295.

Salaün, F., 2016. *Microencapsulation technology for smart textile coatings. Active coatings for smart textiles*. Cambridge: Elsevier.

Shigeta, Y., *et al.*, 2004. Skin whitening effect of linoleic acid is enhanced by liposomal formulations. *Biological & pharmaceutical bulletin*, 27 (4), 591–594.

Singh, M.K., Varun, V., and Behera, B., 2011. Cosmetotextiles: state of art. *Fibres and textiles in Eastern Europe*, 19, 27–33.

Torrado, S., Torrado, J.J., and Cadórniga, R., 1992. Topical application of albumin microspheres containing vitamin A drug release and availability. *International journal of pharmaceutics*, 86 (2–3), 147–152.

Tulloch, A., 1970. The composition of beeswax and other waxes secreted by insects. *Lipids*, 5 (2), 247–258.

Turton, R., and Cheng, X., 2007. Cooling processes and congealing. *Encyclopedia of pharmaceutical technology*, 2, 761–773.

Upadhyay, H., Jahan, S., and Upreti, M., 2016. Cosmetotextiles: emerging trend in technical textiles. *IOSR journal of polymer and textile engineering (IOSR-JPTE)*, 3 (6), 8–14.

Vandenburg, L., and Wilder, E., 1970. The structural constituents of carnauba wax. *Journal of the american oil chemists society*, 47 (12), 514–518.

VARONA, E. & WRIGHT, A. 2005. *Bimodal pore size nonwoven web and wiper*. Google Patents.

Watt, F.M., and Fujiwara, H., 2011. Cell-extracellular matrix interactions in normal and diseased skin. *Cold spring harbor perspectives in biology*, 3 (4), a005124–a005124.

Xiao, Z., *et al.*, 2014. A review of the preparation and application of flavour and essential oils microcapsules based on complex coacervation technology. *Journal of the science of food and agriculture*, 94 (8), 1482–1494.

Yang, J.-H., *et al.*, 2003. Efficient transdermal penetration and improved stability of L-ascorbic acid encapsulated in an inorganic nanocapsule. *Bulletin of the korean chemical society*, 24, 499–503.

Yilmaz, E., & Öndoğan, Z. 2014. Rising trend in functional textiles "cosmetic textiles". *International Izmir Textile and*

*Apparel Symposium,Istanbul, Turkey,* ss.193–195. [Accessed 2 to 5 April 2014].

Yin, W., and Yates, M., 2009. Encapsulation and sustained release from biodegradable microcapsules made by emulsification/freeze drying and spray/freeze drying. *Journal of colloid and interface science*, 336 (1), 155–161.

Yoksan, R., Jirawutthiwongchai, J., and Arpo, K., 2010. Encapsulation of ascorbyl palmitate in chitosan nanoparticles by oil-in-water emulsion and ionic gelation processes. *Colloids and surfaces B: biointerfaces*, 76 (1), 292–297.

Zion, M. R., 2016. Anti-Aging Market (Baby Boomer, Generation X and Generation Y), by product (Botox, Anti-Wrinkle Products, Anti-Stretch Mark Products, and Others), by Services (Anti-Pigmentation Therapy, Anti-Adult Acne Therapy, Breast Augmentation, Liposuction, Chemical Peel, Hair Restoration Treatment, and Others), by Device (Microdermabrasion, Laser Aesthetics, Anti-Cellulite Treatment and Anti-Aging Radio Frequency Devices): Global Industry Perspective, Comprehensive Analysis, Size, Share, Growth, Segment, Trends and Forecast, 2015–2021 (Report Code: ZMR-33). [Online]. Available from: https://www.zionmarketresearch.com/report/anti-aging-market